A unitary transformation approach to the mutual quenching of structural and magnetic ordering in cooperative Jahn-Teller systems

2001 J. Phys.: Condens. Matter 13 1079

(http://iopscience.iop.org/0953-8984/13/5/321)

INSTITUTE OF PHYSICS PUBLISHING JOURNAL OF PHYSICS: CONDENSED MATTER

J. Phys.: Condens. Matter **13** (2001) 1079–1091 www.iop.org/Journals/cm PII: S0953-8984(01)17221-8

A unitary transformation approach to the mutual quenching of structural and magnetic ordering in cooperative Jahn–Teller systems

Kai Ji and H Zheng

Department of Applied Physics, Shanghai Jiao Tong University, Shanghai 200030, People's Republic of China

Received 18 September 2000, in final form 9 November 2000

Abstract

A new approach based on a unitary transformation, the $\boldsymbol{k}$-dependent displacement transformation, is proposed for re-examining the properties of the mutual quenching Jahn–Teller system. We show that when a unitary transformation and the perturbation approximation are applied together to this system, the retardation effect must be considered also. This requirement is fulfilled in our approach, which takes the retardation effect into account through a $\boldsymbol{k}$-dependent function $\delta_{\boldsymbol{k}}$, with the result that the unitary transformation and perturbation approximation work together properly. The order parameters, critical temperatures, and magnetic moment of the system investigated are calculated; they demonstrate that the retardation effect is important near the adiabatic limit, and our approach based on transformation is effective up to this limit.

1. Introduction

The non-Kramers degeneracy of the electron–phonon system is often called the cooperative Jahn–Teller (CJT) effect. Recently, the study of the CJT effect has been flourishing in the fields of high-T_c superconductivity [1] and ferroelectricity [2]; meanwhile numerous theoreticians and experimentalists [3–8] have been engaged in the study of the phase transitions and long-range orderings of the CJT systems. In present paper we carry out a theoretical study of the long-range orderings using a unitary transformation (UT) approach, and investigate the mutual quenching CJT system as an example, to demonstrate the use of our theory.

The Hamiltonian of the system reads (we let $\hbar = 1$ and $k_B = 1$ throughout the paper)

$$H = \frac{1}{2}C_0\Omega U^2 - g_0\sqrt{\frac{C_0\Omega}{N}}U\sum_m \sigma_z^m + \epsilon_0\sum_m I^m + \sum_{\boldsymbol{k}}\omega_{\boldsymbol{k}}b_{\boldsymbol{k}}^\dagger b_{\boldsymbol{k}} - \frac{1}{\sqrt{N}}\sum_{m,\boldsymbol{k}} g_{\boldsymbol{k}}\sigma_z^m(b_{-\boldsymbol{k}}^\dagger + b_{\boldsymbol{k}})\mathrm{e}^{-\mathrm{i}\boldsymbol{k}\cdot\boldsymbol{m}} - \frac{1}{2}\sum_{m,n}\bar{J}_{mn}\sigma_y^m\sigma_y^n - g\mu_B H_z\sum_m \sigma_y^m. \tag{1}$$

0953-8984/01/051079+13$30.00

The first term describes the elastic energy of the crystal, the second term describes the interaction of electrons with the uniform strain U, and the next three terms are the energies of the free electron, the phonon, and the phonon–pseudospin interaction, respectively. The last two terms correspond to the magnetic exchange interaction and the Zeeman interaction under an external magnetic field. N is the number of pseudospins, σ_y^m and σ_z^m the Pauli matrices at site $\boldsymbol{m}$, $b_k^\dagger$ and b_k the creation and annihilation operators for a phonon with frequency ω_k. Ω is the volume of the unit cell, C_0 the 'bare' elastic constant per unit volume, g_0^2 the electron–strain coupling constant, μ_B the Bohr magneton, and g the spectroscopic factor for positive ions.

$$g_k^2 = \frac{\alpha}{2}\omega_0^2/\omega_k$$

and α is the phonon–pseudospin coupling constant, ω_0 is the upper limit of the phonon frequency, $\omega_0 \sim \sqrt{1/M}$, and M is the reduced mass.

Minimizing Hamiltonian (1) with respect to the equilibrium strain, we have

$$U = g_0\sqrt{\frac{N}{C_0\Omega}}\bar{\sigma}_z$$

and the Hamiltonian can be rewritten as

$$H = N\epsilon_0 + \frac{N}{2}g_0^2\bar{\sigma}_z^2 - g_0^2\bar{\sigma}_z\sum_m \sigma_z^m + \sum_m \omega_k b_k^\dagger b_k - \frac{1}{\sqrt{N}}\sum_{m,k} g_k\sigma_z^m(b_{-k}^\dagger + b_k)\mathrm{e}^{-\mathrm{i}k\cdot m} - \frac{1}{2}\sum_{m,n}\bar{J}_{mn}\sigma_y^m\sigma_y^n - g\mu_B H_z\sum_m \sigma_y^m. \tag{2}$$

Since the magnetic exchange interaction is a long-range one, the sixth term of Hamiltonian (2) can be decoupled using the mean-field approximation: $\sigma_y^m\sigma_y^n \approx 2\bar{\sigma}_y\sigma_y^m - \bar{\sigma}_y^2$. But, owing to the electron–phonon coupling in the fifth term, H (equation (2)) cannot yet be diagonalized.

A conventional treatment [3] of this problem starts with the following UT of H (equation (2)):

$$\tilde{H} = \exp(S')H\exp(-S') \tag{3}$$

$$S' = -\frac{1}{\sqrt{N}}\sum_{m,k}\frac{g_k}{\omega_k}(b_{-k}^\dagger - b_k)\sigma_z^m\mathrm{e}^{-\mathrm{i}k\cdot m}. \tag{4}$$

After the transformation,

$$\begin{aligned}\tilde{H} = {} & N\epsilon_0 + \frac{N}{2}g_0^2\bar{\sigma}_z^2 - g_0^2\bar{\sigma}_z\sum_m \sigma_z^m + \sum_m \omega_k b_k^\dagger b_k - \frac{1}{\sqrt{N}}\sum_k\sum_{m,n}\frac{g_k^2}{\omega_k}\sigma_z^m\sigma_z^n\mathrm{e}^{\mathrm{i}k\cdot(m-n)} \\ & - \frac{1}{2}\sum_{m,n}\bar{J}_{mn}[\sigma_y^m\cosh(2g_m) + \mathrm{i}\sigma_x^m\sinh(2g_m)] \\ & \times [\sigma_y^n\cosh(2g_n) + \mathrm{i}\sigma_x^n\sinh(2g_n)] \\ & - g\mu_B H_z\sum_m[\sigma_y^m\cosh(2g_m) + \mathrm{i}\sigma_x^m\sinh(2g_m)]\end{aligned} \tag{5}$$

where

$$g_m = \frac{1}{\sqrt{N}}\sum_k\frac{g_k}{\omega_k}(b_{-k}^\dagger - b_k)\mathrm{e}^{-\mathrm{i}k\cdot m}. \tag{6}$$

The previous coupling in the fifth term of H (equation (2)) is decoupled, but new tangling occurs. Then we apply the perturbation approximation in order to permit the disregarding of

the newly emerged electron–phonon coupling; thus $\cosh(2g_m) \to \gamma_0$, $\sinh(2g_m) \to 0$, and

$$\tilde{H} = N\epsilon_0 + \frac{N}{2}g_0^2\bar{\sigma}_z^2 - g_0^2\bar{\sigma}_z\sum_m \sigma_z^m + \sum_m \omega_k b_k^\dagger b_k - \frac{1}{\sqrt{N}}\sum_k\sum_{m,n}\frac{g_k^2}{\omega_k}\sigma_z^m\sigma_z^n e^{ik\cdot(m-n)} - \frac{\gamma_0^2}{2}\sum_{m,n}\bar{J}_{mn}\sigma_y^m\sigma_y^n - g\mu_B\gamma_0 H_z\sum_m\sigma_y^m \tag{7}$$

where

$$\gamma_0 = \langle p, 0|\cosh(2g_m)|p, 0\rangle = \exp\left[-\frac{2}{N}\sum_k\frac{g_k^2}{\omega_k^2}\right]. \tag{8}$$

$|p, 0\rangle$ is the vacuum state of phonons. Upon making this approximation, the diagonalization of the Hamiltonian becomes possible. Furthermore, as γ_0 can be expanded in powers of g_k^2—that is, γ_0 is connected with the high-order coupling between the electron and phonon—the contribution of the electron–phonon interaction to the electron subsystem is effectively considered via γ_0. On the basis of Hamiltonian (7), Kaplan and Vekhter [3] studied the mutual reduction of structural and magnetic orderings in the cooperative JT system of $HoPO_4$ and $TmVO_4$.

2. Theoretical analysis

2.1. Difficulty

UT is a mathematical technique that does not involve any approximation; the eigenvalue of the original Hamiltonian is invariable under the transformation; the calculation based on the transformed eigenstates is exact. However, when it is used together with other approximation treatments, the results become conditionally correct. To reveal this deviation, we study the Hamiltonians in the adiabatic and antiadiabatic limits.

In the adiabatic limit ($M \to \infty$), the original Hamiltonian (2) becomes

$$H(M\to\infty) = N\epsilon_0 + \frac{N}{2}\left(g_0^2 + \frac{2g_Q^2}{\omega_Q}\right)\bar{\sigma}_z^2 - \left(g_0^2 + \frac{2g_Q^2}{\omega_Q}\right)\bar{\sigma}_z\sum_m\sigma_z^m - \frac{1}{2}\sum_{m,n}\bar{J}_{mn}\sigma_y^m\sigma_y^n - g\mu_B H_z\sum_m\sigma_y^m \tag{9}$$

and in the antiadiabatic limit ($M \to 0$), the Hamiltonian becomes

$$H(M\to 0) = N\epsilon_0 + \frac{N}{2}g_0^2\bar{\sigma}_z^2 - g_0^2\bar{\sigma}_z\sum_m\sigma_z^m + \sum_k\omega_k b_k^\dagger b_k - \frac{1}{N}\sum_k\sum_{m,n}\frac{g_k^2}{\omega_k}\sigma_z^m\sigma_z^n e^{ik\cdot(m-n)} - \frac{1}{2}\sum_{m,n}\bar{J}_{mn}\sigma_y^m\sigma_y^n - g\mu_B H_z\sum_m\sigma_y^m. \tag{10}$$

Both equations (9) and (10) are obtained exactly [9, 10].

In the light of (8), the approximated Hamiltonian (7) in the two extremes should be

$$\tilde{H}(M\to\infty) = N\epsilon_0 + \frac{N}{2}\left(g_0^2 + \frac{2g_Q^2}{\omega_Q}\right)\bar{\sigma}_z^2 - \left(g_0^2 + \frac{2g_Q^2}{\omega_Q}\right)\bar{\sigma}_z\sum_m\sigma_z^m \tag{11}$$

and

$$\tilde{H}(M \to 0) = N\epsilon_0 + \frac{N}{2} g_0^2 \bar{\sigma}_z^2 - g_0^2 \bar{\sigma}_z \sum_m \sigma_z^m + \sum_k \omega_k b_k^\dagger b_k - \frac{1}{N} \sum_k \sum_{m,n} \frac{g_k^2}{\omega_k} \sigma_z^m \sigma_z^n \mathrm{e}^{\mathrm{i}k\cdot(m-n)} - \frac{1}{2} \sum_{m,n} \bar{J}_{mn} \sigma_y^m \sigma_y^n - g\mu_B H_z \sum_m \sigma_y^m. \tag{12}$$

Obviously, the approximated Hamiltonian (7) is consistent with the original Hamiltonian (2) only in the antiadiabatic limit. In the adiabatic limit, the magnetic interaction terms disappear.

We attribute this error to the omission of the retardation effect in the UT. In CJT systems, the localized electrons at different sites correlate with each other through the coupling with the phonons. However, when the mass of the phonon increases, the coupling decreases because the phonon cannot follow the electron instantly. This is the effect of retardation, which is negligible in the antiadiabatic limit, but highly significant in the adiabatic limit. As the UT and perturbation treatment does not take the retardation effect into account, the quantum lattice fluctuation is overestimated near the adiabatic limit, where serious deviation occurs.

2.2. Solution

In order to consider the system from the adiabatic limit to the antiadiabatic limit, we adopt a $\boldsymbol{k}$-dependent displacement transformation [11]. First we let the $\boldsymbol{Q}$-mode phonon be displaced to take into account the long-range phonon ordering:

$$H^* = \exp(R) H \exp(-R) \qquad R = -\sqrt{N} \frac{g_Q}{\omega_Q} (b_{-Q}^\dagger - b_Q) \bar{\sigma}_z \tag{13}$$

where H is the original Hamiltonian (2), $\boldsymbol{k} = \boldsymbol{Q} = (0, 0, 0)$ is the wave vector of ferroelectric ordering which makes $g_{\boldsymbol{k}}^2/\omega_{\boldsymbol{k}}$ maximum. The second UT is a $\boldsymbol{k}$-dependent one:

$$\tilde{H} = \exp(S) H^* \exp(-S) \qquad S = -\frac{1}{\sqrt{N}} \sum_{m,k} \frac{g_k}{\omega_k} \delta_k (b_{-k}^\dagger - b_k) \mathrm{e}^{-\mathrm{i}k\cdot m} (\sigma_z^m - \bar{\sigma}_z). \tag{14}$$

δ_k is a $\boldsymbol{k}$-dependent function and its form will be determined later. We separate $\tilde{H}$ into three parts according to the order of the coupling constant g_k [9, 12]:

$$\tilde{H} = H_0 + H_{I1} + H_{I2} \tag{15}$$

where

$$H_0 = N\epsilon_0 - NV_0 - A\bar{\sigma}_z \sum_m \sigma_z^m + \frac{N}{2} A \bar{\sigma}_z^2 - B \sum_m \sigma_y^m + \sum_k \omega_k b_k^\dagger b_k \tag{16}$$

is the unperturbed Hamiltonian which contains the zeroth-order terms of g_k, and

$$H_{I1} = -\frac{1}{\sqrt{N}} \sum_{m,k} g_k (1 - \delta_k)(\sigma_z^m - \bar{\sigma}_z)(b_{-k}^\dagger + b_k) \mathrm{e}^{-\mathrm{i}k\cdot m} - 2B \sum_m \mathrm{i}\sigma_x^m g_m \tag{17}$$

is the first-order perturbative Hamiltonian which contains the first-order terms of g_k. The second- and higher-order terms of g_k are contained in perturbative Hamiltonian H_{I2}. In equations (16) and (17),

$$A = g_0^2 + 2\left(\frac{g_Q^2}{\omega_Q} - V_0 \right) \tag{18}$$

represents the effective electron–electron interaction originating from both electron–strain and electron–phonon coupling, and

$$B = g\mu_B H_z \gamma_0 + \bar{J}_0 \bar{\sigma}_y \tag{19}$$

represents the effective magnetic interaction originating from Zeeman and exchange interaction. Also,

$$g_m = \frac{1}{\sqrt{N}} \sum_k \frac{g_k}{\omega_k} \delta_k (b_{-k}^\dagger - b_k) \mathrm{e}^{-\mathrm{i}k\cdot m} \tag{20}$$

$$\gamma_0 = \exp\left[-\frac{2}{N} \sum_k \frac{g_k^2}{\omega_k^2} \delta_k^2 \right] \tag{21}$$

$$V_0 = \frac{1}{N} \sum_k \frac{g_k^2}{\omega_k} \delta_k (2 - \delta_k) \tag{22}$$

$$\bar{J}_0 = \gamma_0^2 \sum_n \bar{J}_{mn} \cosh\left[\frac{4}{N} \sum_k \frac{g_k^2}{\omega_k^2} \delta_k^2 \cos \boldsymbol{k} \cdot (\boldsymbol{m} - \boldsymbol{n}) \right]. \tag{23}$$

In equation (14), we insert a $\boldsymbol{k}$-dependent function δ_k to take into account the retardation effect. We assume that δ_k takes the functional form

$$\delta_k = \frac{\omega_k}{\omega_k + 2A}. \tag{24}$$

The reason for this choice will be given later.

Here we show our unperturbed Hamiltonian (16) in the two extremes. When $M \to \infty$ ($\omega_0 \to 0$), g_k^2/ω_k is a finite quantity but δ_k goes to zero. Thus $V_0 = 0$, $\gamma_0 = 1$, and

$$\begin{aligned} H_0(M \to \infty) = N\epsilon_0 + \frac{N}{2}\left(g_0^2 + \frac{2g_Q^2}{\omega_Q} \right) \bar{\sigma}_z^2 - \left(g_0^2 + \frac{2g_Q^2}{\omega_Q} \right) \bar{\sigma}_z \sum_m \sigma_z^m \\ - \left(g\mu_B H_z + \sum_n \bar{J}_{mn} \bar{\sigma}_y \right) \sum_m \sigma_y^m. \end{aligned} \tag{25}$$

We note that if we subject $H(M \to \infty)$ (equation (9)) to the mean-field approximation and rewrite $\sigma_y^m \sigma_y^n$ as $2\bar{\sigma}_y \sigma_y^m - \bar{\sigma}_y^2$, equation (9) will have the same form as equation (25). In the opposite extreme, $M \to 0$ ($\omega_0 \to \infty$), $g_k^2/\omega_k^2 = 0$ and $\delta_k \to 1$. Thus

$$V_0 = \frac{1}{N} \sum_k g_k^2/\omega_k$$

and $\gamma_0 = 1$, and

$$\begin{aligned} H_0(M \to 0) = N\epsilon_0 - NV_0 + \frac{N}{2} A \bar{\sigma}_z^2 - A\bar{\sigma}_z \sum_m \sigma_z^m + \sum_k \omega_k b_k^\dagger b_k \\ - \left(g\mu_B H_z + \sum_n \bar{J}_{mn} \bar{\sigma}_y \right) \sum_m \sigma_y^m. \end{aligned} \tag{26}$$

In equation (10), if we rewrite $\sigma_y^m \sigma_y^n$ and $\sigma_z^m \sigma_z^n$ within the mean-field approximation, then we obtain the same Hamiltonian, $H_0(M \to 0)$ (equation (26)). In this way, we see that our unperturbed Hamiltonian H_0 (equation (16)) is consistent with the original Hamiltonian (2) in both the adiabatic and antiadiabatic limits. In particular, the magnetic elements lost in equation (11) are well retained here. So H_0 (equation (16)) can be regarded as a better unperturbed Hamiltonian for the perturbation approximation.

2.3. Order parameters

As shown in the fifth and sixth terms of the original Hamiltonian (2), the electrons of different sites correlate with each other via two sorts of long-range interaction: pseudospin–phonon coupling and magnetic exchange interaction. These two interactions are the microscopic origins of the competing structural and magnetic orderings in the mutual quenching JT crystals. Therefore, we chose $\langle\sigma_z^m\rangle$ and $\langle\sigma_y^m\rangle$ as the structural and magnetic order parameters, respectively.

We diagonalize H_0, equation (16), by using a unitary matrix $U = \prod_m U_m$, where

$$U_m = \begin{pmatrix} \mathrm{i}u_m & \mathrm{i}v_m \\ -v_m & u_m \end{pmatrix} \tag{27}$$

$$u_m = \sqrt{\frac{E + A\bar{\sigma}_z}{2E}} \qquad v_m = \sqrt{\frac{E - A\bar{\sigma}_z}{2E}} \qquad E = \sqrt{B^2 + A^2\bar{\sigma}_z^2}. \tag{28}$$

The diagonalized form of H_0 is

$$H_0' = U^\dagger H_0 U = N\epsilon_0 - NV_0 + \frac{N}{2}A\bar{\sigma}_z^2 - E\sum_m \sigma_z^m + \sum_k \omega_k b_k^\dagger b_k. \tag{29}$$

The structural order parameter

$$\begin{aligned}\langle\sigma_z^m\rangle &= \frac{\mathrm{Tr}[\exp(-\beta\tilde{H})\sigma_z^m]}{\mathrm{Tr}[\exp(-\beta\tilde{H})]} = \frac{\mathrm{Tr}[\exp(-\beta H_0')(\{B/E\}\sigma_x^m + \{A\bar{\sigma}_z/E\}\sigma_z^m)]}{\mathrm{Tr}[\exp(-\beta H_0')]} \\ &= \frac{A\bar{\sigma}_z}{E}\tanh(\beta E).\end{aligned} \tag{30}$$

Thus $\langle\sigma_z^m\rangle$ can be self-consistently determined from the equation

$$\frac{A}{E}\tanh(\beta E) = 1. \tag{31}$$

The magnetic order parameter is

$$\langle\sigma_y^m\rangle = \frac{\mathrm{Tr}\{\exp(-\beta\tilde{H})[\sigma_y^m\cosh(2g_m) + \mathrm{i}\sigma_x^m\sinh(2g_m)]\}}{\mathrm{Tr}[\exp(-\beta\tilde{H})]} = \frac{B\gamma_T}{E}\tanh(\beta E) \tag{32}$$

where

$$\gamma_T = \langle\cosh(2g_m)\rangle = \exp\left[-\frac{2}{N}\sum_k \frac{g_k^2}{\omega_k^2}\delta_k^2\coth\frac{\beta\omega_k}{2}\right]. \tag{33}$$

Here we have omitted the contributions of the perturbative Hamiltonian and set $\tilde{H} = H_0$ under the perturbation approximation.

2.4. Explanations

From equations (4), (13), and (14) we note that, if we set $\delta_k \equiv 1$, we have

$$S + R = -\frac{1}{\sqrt{N}}\sum_{m,k}\frac{g_k}{\omega_k}(b_{-k}^\dagger - b_k)\sigma_z^m \mathrm{e}^{-\mathrm{i}k\cdot m} = S'.$$

So the previous UT, equations (3) and (4), is just a special case of our k-dependent UT when $\delta_k \equiv 1$. According to equation (24), $\delta_k \equiv 1$ means $\omega_k = \infty$. However, the angular frequency ω_k ($\sim\sqrt{1/M}$) cannot be infinity unless $M = 0$. In the region $0 < M < \infty$, ω_k must be a finite quantity; that is, the phonons vibrate with finite frequencies and cannot follow the pseudospins instantly. If we take $\delta_k \equiv 1$, the retardation effect is omitted; as a result the quantum lattice

fluctuation is overestimated and the phonon dressing effect [11] is underestimated. That is why UT (3), (4) gives the incorrect Hamiltonian (7). Therefore, δ_k as well as the UT should take a k-dependent form so as to take into account the retardation effect.

Now we say something about the choice of δ_k. The perturbative Hamiltonian H_{I1} (equation (17)) can be transformed as

$$H'_{I1} = U^{\dagger}H_{I1}U = -\frac{1}{\sqrt{N}}\sum_{m,k} g_k \mathrm{e}^{-\mathrm{i}k\cdot m}\left\{(1-\delta_k)\left(\frac{A}{E}\sigma_z^m - 1\right)\bar{\sigma}_z(b_{-k}^{\dagger} + b_k) + \frac{\delta_k}{\omega_k}B\left[\left(\frac{A}{E}-1\right)(\sigma_+^m b_k + \sigma_-^m b_{-k}^{\dagger}) + \left(\frac{A}{E}+1\right)(\sigma_+^m b_{-k}^{\dagger} + \sigma_-^m b_k)\right]\right\}. \quad (34)$$

Allowing for equation (31), the thermodynamical average of the factor $(A/E)\sigma_z^m - 1$ in the first term of H'_{I1} is zero because

$$\langle\sigma_z^m\rangle_0 = \tanh(\beta E) \qquad \langle\cdots\rangle_0 = \mathrm{Tr}[\exp(-\beta H'_0)\cdots]/\mathrm{Tr}[\exp(-\beta H'_0)]. \quad (35)$$

The reason for introducing the functional form of δ_k is that, when $T = 0$ $(A/E = 1)$, the term $\sigma_+^m b_k + \sigma_-^m b_{-k}^{\dagger}$ in H'_{I1} disappears. Also, $(\sigma_+^m b_{-k}^{\dagger} + \sigma_-^m b_k)|g_0\rangle = 0$ ($|g_0\rangle$ is the ground state of H'_0).

3. Numerical calculations and discussion

As shown in equation (24), δ_k is a function of the wave vector k and varies within $0 \leqslant \delta_k \leqslant 1$. In the numerical calculation, the value of δ_k is not given arbitrarily, but self-consistently determined from equations (18), (22), and (24).

We adopt a three-dimensional simple cubic lattice for the numerical calculation with the phonon frequency

$$\omega_k = \omega_0\sqrt{1-\rho(1+\xi_k)/2} \qquad -\pi \leqslant k_x, k_y, k_z \leqslant \pi \quad (36)$$

where $\xi_k = (\cos k_x + \cos k_y + \cos k_z)/3$ and ρ measures the size of the phonon dispersion. As all the k-dependence in the calculation arises through the frequency ω_k, we can introduce the density of states (DOS) $N(\omega)$:

$$N(\omega) = \sum_k \delta(\omega - \omega_k) = \int_{-1}^{1} \mathrm{d}\xi\ N_\xi(\xi)\delta(\omega - \omega_0\sqrt{1-\rho(1+\xi)/2}) \quad (37)$$

where

$$N_\xi(\xi) = \sum_k \delta(\xi - \xi_k)$$

is the DOS for ξ_k. For simplicity, we assume that $N_\xi(\xi) = 2\sqrt{1-\xi^2}/\pi$ is an elliptic DOS. Hence, we have

$$N(\omega) = \frac{8\omega}{\pi\rho\omega_0^2}\left\{1 - \left[1 - \frac{2}{\rho}\left(1 - \left(\frac{\omega}{\omega_0}\right)^2\right)\right]^2\right\}^{1/2} \quad (38)$$

for the region $\omega_0\sqrt{1-\rho} < \omega < \omega_0$. Outside the region, $N(\omega) = 0$.

In figures 1(a) and 1(b), we plot the order parameters $\langle\sigma_y^m\rangle$ and $\langle\sigma_z^m\rangle$ as functions of the external magnetic field H_z, respectively. The solid lines are calculated by differentiating the free energy F (see the appendix), and hence include the contributions of the perturbative Hamiltonian $H_{I1} + H_{I2}$ up to second-order terms. The solid dots show the results of our theory approximating $\tilde{H}$ as H_0, and the dashed lines are the results of the theory for $\delta_k \equiv 1$. The consistency of the solid dots with the solid lines indicates that our theory gives a better unperturbed Hamiltonian H_0 and that the contribution of $H_{I1} + H_{I2}$ is actually very small. So we set $\tilde{H} = H_0$ in the following discussion.

We investigate the system in two cases: external magnetic field $H_z = 0$ and $H_z > 0$.

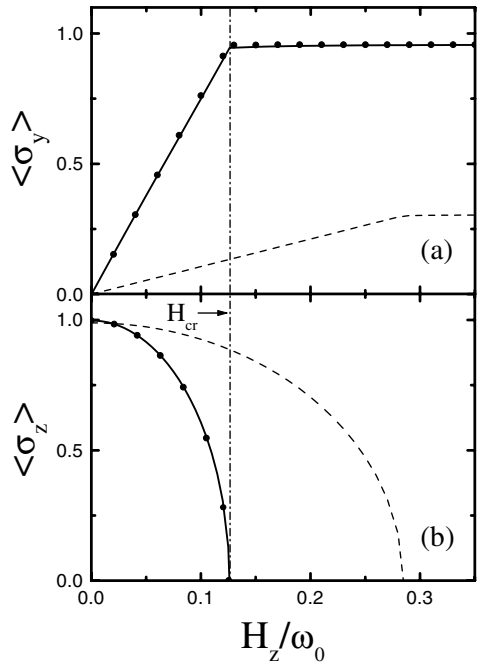

Figure 1. Order parameters versus external magnetic field strength H_z/ω_0 when $g_0^2/\omega_0 = 1$, $\alpha/\omega_0 = 0.5$, $T/\omega_0 = 0.5$, and $J_1/\omega_0 = 0.1$. (a) Variation of the magnetic order parameter $\langle\sigma_y^m\rangle$. (b) Variation of the structural order parameter $\langle\sigma_z^m\rangle$. H_{cr} denotes the critical H_z at which the structural ordering disappears. Solid lines: results including the contributions of the perturbation $H_{I1} + H_{I2}$ up to the second-order terms; solid dots: results from our theory setting $\tilde{H} = H_0$; dashed lines: results from the theory with $\delta_k \equiv 1$.

3.1. $H_z = 0$

According to equations (31) and (32), three phases exist when $H_z = 0$.

(a) When $\bar{J}_0\gamma_T > A$, magnetic ordering is dominant, the magnetic parameter $\bar{\sigma}_y = \gamma_T \tanh(\beta\bar{J}_0\bar{\sigma}_y)$, and the structural parameter $\bar{\sigma}_z = 0$. The prototypical crystal of this kind is $HoPO_4$.
(b) When $\bar{J}_0\gamma_T < A$, structural ordering arises: $\bar{\sigma}_z = \tanh(\beta A\bar{\sigma}_z)$, but $\bar{\sigma}_y = 0$. This type of ordering exists in $TmVO_4$.
(c) When temperature is high enough, no ordering remains and the system is in a disordered phase.

Figure 2 is the phase diagram for the case where $H_z = 0$, where T_c, T_m, and T_s are critical temperatures, and J_1 is the nearest-neighbour exchange constant (the nearest-neighbour approximation is applied in this section). The solid lines represent our results and dashed lines the theory with $\delta_k \equiv 1$. The difference between the two theories is obvious and mainly results from the disparity as regards T_m. Our curve for T_m is quite flat, while the theory with $\delta_k \equiv 1$ gives a declining one. This is because the theory with $\delta_k \equiv 1$ loses the magnetic elements in its deformed Hamiltonian.

When the system is in the magnetic phase, the magnetic parameter $\bar{\sigma}_y > 0$, so we have an on-site magnetic moment $\mu = g\mu_B\gamma_T \tanh(\bar{J}_0\mu/g\mu_B k_B T)$. In figure 3, we plot μ/μ_m as a function of J_1/α at $T = 0$. $\mu_m = \mu|_{\omega\to\infty}$ is used as a renormalization factor. The solid

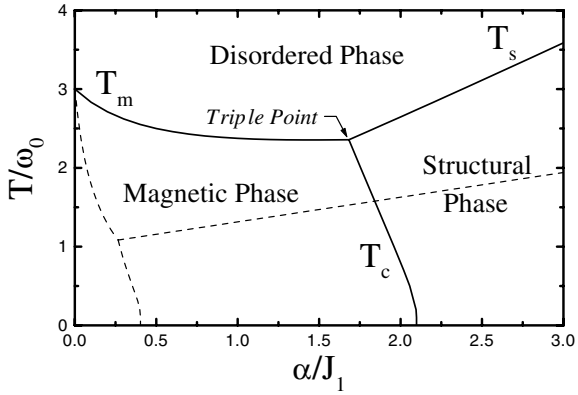

Figure 2. The critical temperature T/ω_0 versus α/J_1 phase diagram. $H_z = 0$, $g_0^2/\omega_0 = 1$, and $J_1/\omega_0 = 0.5$. Solid line: our theory; dashed line: the theory with $\delta_k \equiv 1$.

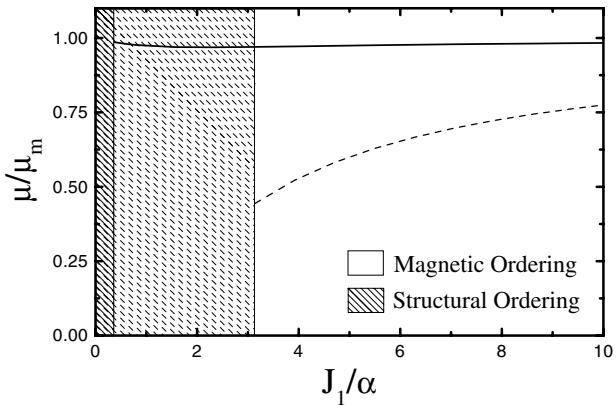

Figure 3. Site magnetic moment μ/μ_m versus J_1/α. $T = 0$, $g_0^2/\omega_0 = 1$, and $J_1/\omega_0 = 1.57$. Solid line: our theory; dashed line: the theory with $\delta_k \equiv 1$.

line is the result from our theory, and the dashed line that from the theory with $\delta_k \equiv 1$. It was once believed that the site magnetic moment μ was significantly reduced by strong phonon–pseudospin interaction α/J_1 [3], as shown by the dashed line. But our theory proves that, due to the retardation effect, a significant reduction is impossible even if $\alpha/J_1 \to \infty$. The reason is the same as for figure 2: the theory with $\delta_k \equiv 1$ underestimates the magnetic interaction.

3.2. $H_z > 0$

In this case, as shown in figures 1(a) and 1(b), the structural ordering can be replaced by a magnetic one with the support of H_z; hence the external magnetic field complicates the competition between the two orderings. Magnetic ordering always exists because the crystals are magnetized by the magnetic field and the on-site magnetic moment $\mu > 0$ ($\bar{\sigma}_y > 0$). Also, structural ordering occurs when $\bar{J}_0\gamma_T < A$ and $H_z < H_{cr}$, corresponding to a phase with coexisting magnetic and structural ordering. Here H_{cr} is the critical value of H_z which is strong enough to remove structural ordering. So there are two phases in this case: the single magnetic phase and the coexistence phase.

When $\bar{\sigma}_z \to 0$, we have $\tanh(\beta E) = g H_{cr}\gamma_0/(A - \bar{J}_0\gamma_T)$, from which we determine H_{cr}. In the phase diagram in figure 4, we plot H_{cr} as a function of J_1. The solid line represents the result from our theory, and the dashed line that from the theory with $\delta_k \equiv 1$. We note that, given the same J_1/ω_0, the theory with $\delta_k \equiv 1$ needs a stronger magnetic field to remove structural ordering; this is also because of its underestimation of the magnetic interaction.

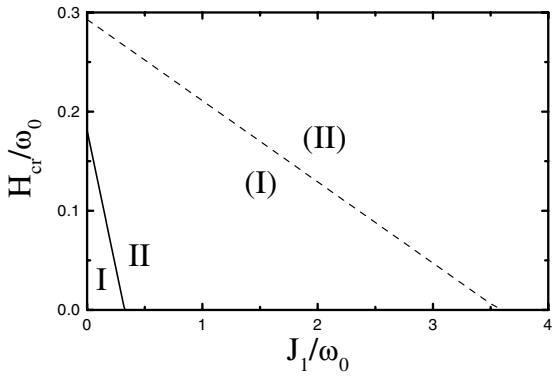

Figure 4. The critical magnetic field strength H_{cr}/ω_0 versus J_1/ω_0 phase diagram. $g_0^2/\omega_0 = 1$, $\alpha/\omega_0 = 0.5$, and $T/\omega_0 = 0.5$. I: coexistence phase; II: magnetic phase. Solid line and areas I, II: our theory; dashed line and areas (I), (II): the theory with $\delta_k \equiv 1$.

The relation between H_{cr} and T is plotted in figure 5. The solid line and dashed line correspond to the results from our theory and the theory with $\delta_k \equiv 1$, respectively. Just like in figure 4, a stronger H_{cr} is required for the theory with $\delta_k \equiv 1$. When $H_z \to 0$, the theory with $\delta_k \equiv 1$ leads to a lower critical temperature T_s separating the structural phase and the disordered phase, which is in accord with the result of figure 2.

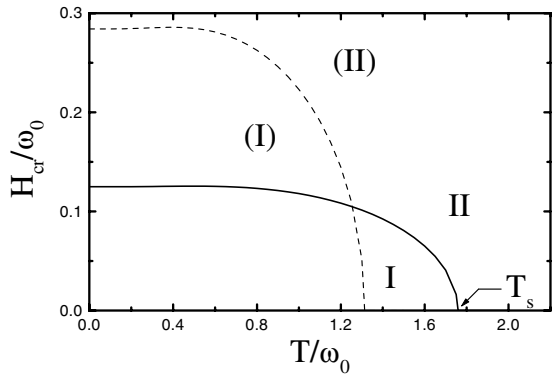

Figure 5. The critical magnetic field strength H_{cr}/ω_0 versus T/ω_0 phase diagram. $g_0^2/\omega_0 = 1$, $\alpha/\omega_0 = 0.5$, and $J_1/\omega_0 = 0.1$. I: coexistence phase; II: magnetic phase. Solid line and areas I, II: our theory; dashed line and areas (I), (II): the theory with $\delta_k \equiv 1$.

4. Conclusions

In this paper, we theoretically studied the mutual quenching Jahn–Teller system using the following procedure:

(1) Apply a $\boldsymbol{k}$-dependent displacement transformation to the original Hamiltonian H to take into account the retardation effect.
(2) Divide the transformed Hamiltonian into unperturbed and perturbative Hamiltonians by means of perturbation theory.
(3) Consider the system on the basis of the unperturbed Hamiltonian H_0.

The central concern of this paper is how to get a good unperturbed Hamiltonian. We show that the retardation effect is important. After taking it into account, our unperturbed Hamiltonian H_0 works well from the adiabatic to the antiadiabatic limit.

The new approach of $\boldsymbol{k}$-dependent displacement transformation which is developed in this paper has the following applications and significance:

(a) It enables the theoretical analysis of the mutual quenching JT system from the adiabatic to the antiadiabatic limit. This approach can also be applied to other cooperative JT and pseudospin–phonon systems.
(b) The new transformation has a sound physical content: the $\boldsymbol{k}$-dependent function $\delta_{\boldsymbol{k}}$ represents the retardation effect of the electron–phonon interaction.
(c) We show that the cooperative JT system displays different features in the adiabatic and the antiadiabatic limits as well as in the intermediate domain. These features were confused in previous works. We are able to tell them apart and give a complete description with the aid of this new approach.

In the framework of the $\boldsymbol{k}$-dependent displacement transformation, we have re-examined the properties of the mutual quenching JT system. Our results are different from the previous ones, especially as regards the critical temperature T_m and the magnetic moment μ. As shown in figures 2 and 3, the two variables should change little according to our theory; however, the theory with $\delta_{\boldsymbol{k}} \equiv 1$ predicts an appreciable decline in them. We believe that our theory has disclosed the real nature of the system, and anticipate further support from experimental observation.

Appendix

In equations (30) and (32) we calculate the order parameters by approximating $\tilde{H}$ as H_0. If more accuracy is desired, the order parameters may be represented through the differentiation of the free energy F. In perturbation theory, F can be calculated as follows [13]:

$$-\beta(F-F_0) = -\int_0^\beta \mathrm{d}\tau\ \langle H'_{I1}(\tau)\rangle_0 + \int_0^\beta \mathrm{d}\tau_1 \int_0^{\tau_1} \mathrm{d}\tau_2\ \langle [H'_{I1}(\tau_1)H'_{I1}(\tau_2)]\rangle_0 - \int_0^\beta \mathrm{d}\tau\ \langle H'_{I2}(\tau)\rangle_0 + \mathrm{O}(g_{\boldsymbol{k}}^3) \tag{A.1}$$

where F_0 is the free energy of H'_0, and $H'_{I1}(\tau) = \exp(H'_0\tau)H'_{I1}\exp(-H'_0\tau)$ holds in the interaction picture.

The order parameters are

$$\langle\sigma_y^m\rangle = \frac{B\gamma_0}{E} - \frac{A\bar{\sigma}_z}{E}\langle\sigma_x^m\rangle' + \langle \mathrm{i}\sigma_y^m \sinh(2g_m)\rangle' + \frac{B\gamma_0}{E}\langle\sigma_z^m[\cosh(2g_m)-\gamma_0]\rangle' - \frac{A\bar{\sigma}_z}{E}\langle\sigma_x^m[\cosh(2g_m)-\gamma_0]\rangle' \tag{A.2}$$

$$\langle\sigma_z^m\rangle = \frac{B}{E}\langle\sigma_x^m\rangle' + \frac{A\bar{\sigma}_z}{E}\langle\sigma_z^m\rangle' \tag{A.3}$$

where

$$\begin{aligned}&\langle\cdots\rangle' = \mathrm{Tr}[\exp(-\beta H')\cdots]/\mathrm{Tr}[\exp(-\beta H')]\\&H' = U^{\dagger}\tilde{H}U = H_0' + H_{I1}' + H_{I2}'.\end{aligned} \tag{A.4}$$

$\langle\sigma_z^m\rangle'$ and $\langle\sigma_x^m\rangle'$ can be calculated by means of differentiation:

$$\langle\sigma_z^m\rangle' = -\frac{1}{N}\frac{\partial}{\partial h_z}F(h_z,h_x)\bigg|_{h_z=0,h_x=0} \qquad \langle\sigma_x^m\rangle' = -\frac{1}{N}\frac{\partial}{\partial h_x}F(h_z,h_x)\bigg|_{h_z=0,h_x=0}. \tag{A.5}$$

For calculating $F(h_z,h_x)$, we let

$$H_0' = N\epsilon_0 - NV_0 + \frac{N}{2}A\bar{\sigma}_z^2 + \sum_{\boldsymbol{k}}\omega_{\boldsymbol{k}}b_{\boldsymbol{k}}^{\dagger}b_{\boldsymbol{k}} - \sum_{\boldsymbol{m}}(E+h_z)\sigma_z^{\boldsymbol{m}} - \sum_{\boldsymbol{m}}h_x\sigma_x^{\boldsymbol{m}}. \tag{A.6}$$

The results are

$$\begin{aligned}\langle\sigma_y^{\boldsymbol{m}}\rangle = \frac{B\gamma_0}{E}\tanh(\beta E)\Bigg\{&1 - \frac{2}{N}\sum_{\boldsymbol{k}}\frac{g_{\boldsymbol{k}}^2}{\omega_{\boldsymbol{k}}}(1-\delta_{\boldsymbol{k}})^2\frac{\beta\bar{\sigma}_z^2}{\sinh^2(\beta E)}\left[1-\frac{\coth(\beta E)}{\beta E}\right]\\&+(\gamma_T-\gamma_0)\left[\frac{\beta B^2}{E^2}\frac{g\mu_B H_z\gamma_0}{\cosh^2(\beta E)} + \frac{g\mu_B H_z\gamma_0}{E}\bar{\sigma}_z^2\cosh(\beta E) + \frac{B}{E}\tanh(\beta E)\right]\\&+(\bar{J}_T-\bar{J}_0)\frac{B\gamma_0}{E}\left[\frac{\beta B}{E}\frac{\tanh(\beta E)}{\cosh^2(\beta E)} - \bar{\sigma}_z^2\right]\\&+f_1 - A\bar{\sigma}_z^2\coth^2(\beta E)f_2 + \frac{E\gamma_T}{\gamma_0}f_3\Bigg\}\end{aligned} \tag{A.7}$$

$$\begin{aligned}\langle\sigma_z^{\boldsymbol{m}}\rangle = \bar{\sigma}_z\Bigg\{&1 - \frac{2}{N}\sum_{\boldsymbol{k}}\frac{g_{\boldsymbol{k}}^2}{\omega_{\boldsymbol{k}}}\frac{(1-\delta_{\boldsymbol{k}})^2}{\sinh^2(\beta E)}\left[\beta\bar{\sigma}_z^2 + \frac{B^2}{AE^2}\right] + (\gamma_T-\gamma_0)\frac{B}{E^2}\left[\frac{2\beta E}{\sinh(2\beta E)} - 1\right]\\&+(\bar{J}_T-\bar{J}_0)\frac{B^2\tanh(\beta E)}{E^3}\left[\frac{2\beta E}{\sinh(2\beta E)} - 1\right] + f_1 - \frac{B^2\coth(\beta E)}{E}f_2\Bigg\}\end{aligned} \tag{A.8}$$

where

$$\bar{J}_T = \gamma_T^2\sum_{\boldsymbol{n}}\bar{J}_{mn}\cosh\left[\frac{4}{N}\sum_{\boldsymbol{k}}\frac{g_{\boldsymbol{k}}^2}{\omega_{\boldsymbol{k}}^2}\delta_{\boldsymbol{k}}^2\cos\boldsymbol{k}\cdot(\boldsymbol{m}-\boldsymbol{n})\right] \tag{A.9}$$

$$\begin{aligned}f_1 = \frac{4}{N}\sum_{\boldsymbol{k}}\frac{g_{\boldsymbol{k}}^2\delta_{\boldsymbol{k}}^2}{\omega_{\boldsymbol{k}}^2}B^2\Bigg\{&\frac{[\coth(\beta E)+1]^2}{\omega_{\boldsymbol{k}}-2E}\left[\frac{\coth(\beta E)-\coth(\beta\omega_{\boldsymbol{k}}/2)}{\omega_{\boldsymbol{k}}-2E} - \frac{\beta\coth(\beta\omega_{\boldsymbol{k}}/2)}{\sinh(2\beta E)}\right]\\&-\frac{[\coth(\beta E)-1]^2}{\omega_{\boldsymbol{k}}+2E}\left[\frac{\coth(\beta E)+\coth(\beta\omega_{\boldsymbol{k}}/2)}{\omega_{\boldsymbol{k}}+2E} - \frac{\beta\coth(\beta\omega_{\boldsymbol{k}}/2)}{\sinh(2\beta E)}\right]\Bigg\}\end{aligned} \tag{A.10}$$

$$\begin{aligned}f_2 = \frac{4}{N}\sum_{\boldsymbol{k}}\frac{g_{\boldsymbol{k}}^2\delta_{\boldsymbol{k}}^2}{\omega_{\boldsymbol{k}}^2}\Bigg\{&\frac{\coth(\beta E)+1}{\omega_{\boldsymbol{k}}-2E}[\coth(\beta E)-\coth(\beta\omega_{\boldsymbol{k}}/2)]\\&+\frac{\coth(\beta E)-1}{\omega_{\boldsymbol{k}}+2E}[\coth(\beta E)+\coth(\beta\omega_{\boldsymbol{k}}/2)]\Bigg\}\end{aligned} \tag{A.11}$$

$$\begin{aligned}f_3 = \frac{4}{N}\sum_{\boldsymbol{k}}\frac{g_{\boldsymbol{k}}^2\delta_{\boldsymbol{k}}^2}{\omega_{\boldsymbol{k}}^2}\Bigg\{&\frac{\coth(\beta E)+1}{\omega_{\boldsymbol{k}}-2E}[\coth(\beta E)-\coth(\beta\omega_{\boldsymbol{k}}/2)]\\&-\frac{\coth(\beta E)-1}{\omega_{\boldsymbol{k}}+2E}[\coth(\beta E)+\coth(\beta\omega_{\boldsymbol{k}}/2)]\Bigg\}.\end{aligned} \tag{A.12}$$

Here all the second-order contributions have been taken into account. And when $T = 0$,

$$\langle \sigma_y^m \rangle = \frac{B\gamma_0}{E} \qquad \langle \sigma_z^m \rangle = \bar{\sigma}_z. \tag{A.13}$$

So the second-order contributions ($O(g_{\boldsymbol{k}}^2)$) become zero when $T = 0$.

The numerical results from equations (A.7) and (A.8) are plotted in figures 1(a) and 1(b), respectively.

References

[1] Bednorz J G and Müller K A 1988 *Rev. Mod. Phys.* **60** 585
[2] Bersuker I B and Polinger V Z 1989 *Vibronic Interactions in Molecules and Crystals* (Berlin: Springer)
[3] Kaplan M D and Vekhter B G 1995 *Cooperative Phenomena in Jahn–Teller Crystals* (New York: Plenum)
[4] Gehring G A and Gehring K A 1976 *Rep. Prog. Phys.* **38** 1
[5] Kaplan M D and Vasilyev A V 1992 *Physica* B **179** 65
[6] Kaplan M D, Perry C H, Cardarelly D and Zimmerman G O 1994 *Physica* B **194** 1453
[7] Kaplan M D and Zimmerman G O 1995 *Phys. Rev.* B **52** 1
[8] Kaplan M D and Zimmerman G O 1997 *Phys. Rev.* B **56** 5193
[9] Zheng H 2000 *Phys. Rev.* B **61** 1088
[10] Hirsch J E and Fradkin E 1983 *Phys. Rev.* B **27** 4302
[11] Zheng H and Zhu S Y 1996 *Phys. Rev.* B **54** 1439
[12] Moore M A and Williams H C W L 1972 *J. Phys. C: Solid State Phys.* **5** 3168
Moore M A and Williams H C W L 1972 *J. Phys. C: Solid State Phys.* **5** 3185
Moore M A and Williams H C W L 1972 *J. Phys. C: Solid State Phys.* **5** 3222
[13] Mahan G D 1990 *Many-Particle Physics* (New York: Plenum) ch 3